



Design considerations for elastomeric normally closed microfluidic valves

Ritika Mohan^a, Benjamin R. Schudel^a, Amit V. Desai^a, Joshua D. Yearsley^c,
Christopher A. Applett^{b,c}, Paul J.A. Kenis^{a,*}

^a Department of Chemical & Biomolecular Engineering, University of Illinois at Urbana-Champaign, Urbana, IL 61801, USA

^b Sandia National Laboratories, Albuquerque, NM 87185, USA

^c Department of Chemical & Nuclear Engineering, University of New Mexico, Albuquerque, NM 87131, USA

ARTICLE INFO

Article history:

Received 28 June 2011

Received in revised form

12 September 2011

Accepted 17 September 2011

Available online 22 September 2011

Keywords:

Microvalves

Soft lithography

Actuation pressure

Hysteresis

Normally closed valves

ABSTRACT

The ease of fabrication and integration of pneumatic microvalves has enabled extensive miniaturization of microfluidic devices capable of performing massively parallel operations. These valves in their typical open configuration, also known as normally open (NO) valves, require to be actuated to remain closed. As a result, devices employing these valves have limited portability in applications that require valves to be closed continuously. Normally closed (NC) valves based on pneumatic actuation not only address the above issue of portability, but also retain the ease of integrating massively parallel networks of microfluidic elements. In this paper, we report the design and fabrication of elastomeric NC microvalves, along with systematic experimental characterization of NC valve operation. Geometrical parameters of the valve, including shape, fluid channel width, membrane thickness, and valve asymmetry, were examined with the objective of minimizing actuation pressures and ensuring reliable operation. We observed that introduction of asymmetry in the valve geometry created points of weak adhesion between the valve and the substrate, which facilitated opening of the valve at lower actuation pressures. Specifically, valves with a sharp corner feature (v-shaped) actuated at lower pressures (1.5 psi) compared to straight-shaped valves (3 psi). We also observed that membrane thickness does not significantly influence the actuation pressures. An important requirement for microfluidic devices using NC valves is selective irreversible bonding of the fluid layer to the substrate, which we achieved by plasma sealing of the fluid layer to the substrate while simultaneously actuating the valves. Based on our experimental observations, we formulated a set of design considerations with the objective of minimizing actuation pressures, ensuring reliable operation, and facilitating convenient integration into complex microfluidic devices. These NC valves have significant potential in applications where portability is highly desired, such as in on-chip analysis, crystallization screening, and in the study of chemical or biological processes over long durations of time.

© 2011 Elsevier B.V. All rights reserved.

1. Introduction

Miniaturization of various microfluidic components and their integration into dense networks is crucial to enable massively parallel operations on a single device. Fine control is required for a variety of applications where small volumes of fluids (picoliters to nanoliters) are manipulated and mixed [1–4]. Microvalves that route flow are probably one of the most important components in these microfluidic devices. Although significant progress has been made in improving the performance of valves with respect to their response time, leakage, dead volume, power consumption, sensitivity to particulate contamination, and chemical compatibility, further improvements are needed [5,6].

A new type of valve that incorporates most or all the above ideal characteristics is highly desired. For instance, elastomeric pneumatic microvalves [7] have been successfully used in many applications that require multi-step and high throughput operations on a single device [1,4]. A significant advantage of these pneumatic microvalves is that the fabrication of the valves is compatible with standard soft lithographic techniques, allowing easy integration of these valves into complex microfluidic devices.

Pneumatic microvalves can be broadly classified into two types: normally open (NO) and normally closed (NC) [2], similar to fail-close and fail-open valve architecture at larger scale systems [8]. Although NO valves are widely used in many microfluidic applications [9,10], devices employing these NO valves have limited portability in applications that require continuous closed state for operation, as these valves need bulky ancillaries (pumps, nitrogen gas cylinders, pneumatic peripherals) for actuation. For example, in our investigations of on-chip protein–antibody interactions [11]

* Corresponding author. Tel.: +1 217 265 0523.

E-mail address: kenis@illinois.edu (P.J.A. Kenis).

or virus detection [12], the valves need to be open only for a short period of time when the solutions are being mixed. Use of NO valves in these applications would have hampered portability between the mixing station and detection ancillaries such as a microscope [11,12]. NC valves not only address the above limitation of restricted portability, but also retain the ease of fabrication and integration into microfluidic devices. Moreover, NO microvalves typically require actuation pressures of 6–30 psi [13,14], whereas NC valves can be actuated with lower pressures, in the range of 1–12 psi, as demonstrated here and by Grover et al. [15].

NC valves made out of silicon and glass have been used in several applications, such as portable fuel cell systems using piezoelectric valves [16] and bidirectional gas regulators for micro-gas chromatography systems [17]. The focus of this paper will be on NC valves made out of elastomeric materials, such as polydimethylsiloxane (PDMS), a commonly used material in microfluidics. Valves made out of elastomeric materials are typically easier to fabricate and actuate at lower pressures. Elastomeric NC valves have been used previously in different microfluidic applications, including cell sorting [18], on-chip electrophoresis [1], combinatorial protein–antibody interaction screening [8], virus detection [12] and on-chip chemical synthesis [19,20]. Some of these NC valves have been characterized for pumping of fluids for a range of flow rates (0–400 nL/s) and operating pressures (0–30 kPa) [21]. None of these studies, however, have specifically focused on design rules to optimize the performance of NC valves, in particular with respect to minimizing their actuation pressures and optimizing their reliability.

Formulation of a set of design rules for these microvalves is important because the actuation of these microvalves involves complex interplay between (i) mechanical deformation of the membrane and (ii) adhesion forces between hard and soft materials, which cannot be quantified easily due to the hysteresis that appears when polymeric substrates contact a stiffer surface. In addition, design rules are needed for devices with dense networks of channels because pressure losses across the device may cause failure of the valves that are furthest away from the actuation pressure source. Hence, design rules are needed that will aid in minimizing actuation pressures for these cases. Furthermore, the design rules will enable fabrication of valves with dimensions that can be easily achieved with standard soft lithography.

2. Materials and methods

2.1. Fabrication of microfluidic devices with NC valves

We fabricated microfluidic devices with NC valves using standard procedures for PDMS-based multi-layer soft lithography [7]. The fabricated two-layer devices consisted of (a) a control layer composed of microchannels that act as pneumatic lines for applying negative pressure and (b) a fluid layer composed of microchannels. RTV 615 poly(dimethyl siloxane) (PDMS) was obtained from General Electric Company (Waterford, NY). Negative photoresists, SU-8 250 and SU-8 25, were obtained from MicroChem Corporation (Newton, MA). (Tridecafluoro-1,1,2,2-tetrahydrooctyl)trichlorosilane was obtained from Gelest, Inc. (Morrisville, PA). The thickness of the photoresist and PDMS layers were measured using Dektak 3030. Negative patterns of the features of the fluid layer and the control layer were patterned on silicon using 20–25 μm thick negative photoresist. Then, a silane monolayer was evaporated onto the silicon masters to prevent the covalent adhesion of PDMS to the silicon substrates. Next, a thin layer of 15:1 PDMS (weight ratio of polymer to cross-linker) was spun on the fluid layer master, 5:1 PDMS was poured on to the control layer master to a thickness of 2 mm, and the two layers

were partially cured at 65 °C for approximately 30 min. The thickness of the valve membrane in the fluid layer was controlled by the spin speed ranging from 1000 to 2000 rpm, yielding 20–60 μm layer thicknesses. After partial curing, the control layer mold was removed from the master, holes were punched for the inlets and outlets of the control layer using a 20 gauge needle (B-D Precision Slide), and the control layer mold was aligned manually with the fluid layer under an optical microscope (Leica MZ6). The aligned layers were further cured at 65 °C for approximately 12 h to yield the final assembled device. The device was then peeled off the fluid layer master, and holes were punched into the fluid layer using a 20 gauge needle. For experiments studying the reversibly sealed nature of the PDMS devices, the device was placed onto a clean glass substrate by simply bringing the PDMS assembled mold and the glass into contact. We chose a glass substrate, as glass is the most commonly used substrate in microfluidic devices when the channels are fabricated out of PDMS [22,23]. Since the objective of the research presented here was to study the influence of valve geometry on actuation pressures, we did not modify the material properties of PDMS.

2.2. Selective irreversible bonding of the PDMS device to glass

In some of the experiments, the PDMS device was irreversibly bonded to glass. In this case, the surface of the assembled device that had the microfluidic features and the glass substrate were treated with atmospheric plasma consisting of oxygen and helium (1:75 volumetric ratio) using a plasma pen (Surfx technologies, Atomflo™ plasma) at 80 W for 2–4 s. After the plasma treatment, all NC valves were actuated so that the valve stops do not touch the glass substrate during bonding, and the PDMS device and the glass were brought into contact. The valves were left actuated for approximately 6–8 h, after which the PDMS device was irreversibly bonded to glass only in the channel areas.

2.3. Actuation of the NC valves in microfluidic devices

Negative pressure was applied to the NC valves using a pump (GastDOA-P704-AA VacuumPump1/8 HP 115 VAC), and the actuation pressures of the microvalves were measured using a pressure controller (Cole Parmer, model 68027-78); the schematic illustration of the set-up is shown in [supplementary information, Fig. S1](#). The valve actuation was performed under an optical microscope (Leica M205) to confirm opening of the valve. Note that the valve is open and will allow fluid flow, when the valve stop is lifted off from the substrate. However, this partial opening of the valve cannot be ascertained by visualizing the device from the top ([Fig. 1\(c\)](#)). Hence, we define the open state of the valve based on formation of contact lines. Two sets of contact lines appear upon actuation, one due to gradual delamination of the valve stop and side walls of the fluid channel, and one due to adhesion of the valve membrane to the roof of the control channel. Specifically, the valve is defined as ‘completely’ open when at least one of the two contact lines (typically circular or oval in shape) links the two opposite edges of the valve stop ([Fig. 1\(c\)](#)). We thus define ‘actuation pressure’ as the pressure required to completely open the valve, based on our definition of ‘completely’ open valve. After testing 8 different devices, we observed that the actuation pressures for all the valves were in the range of 1–6 psi. The standard deviation for actuation pressures for valves with identical geometries (same dimensions) on different devices was ± 0.15 psi, which we represent as 0.3 psi error bars in [Fig. 3](#). This implies that the device-to-device variability resulted in a 0.3 psi variation in actuation pressures. Each valve on the same device was tested in triplicate, and we observed that the actuation pressures for that same valve were within 0.01 psi. Note that all the

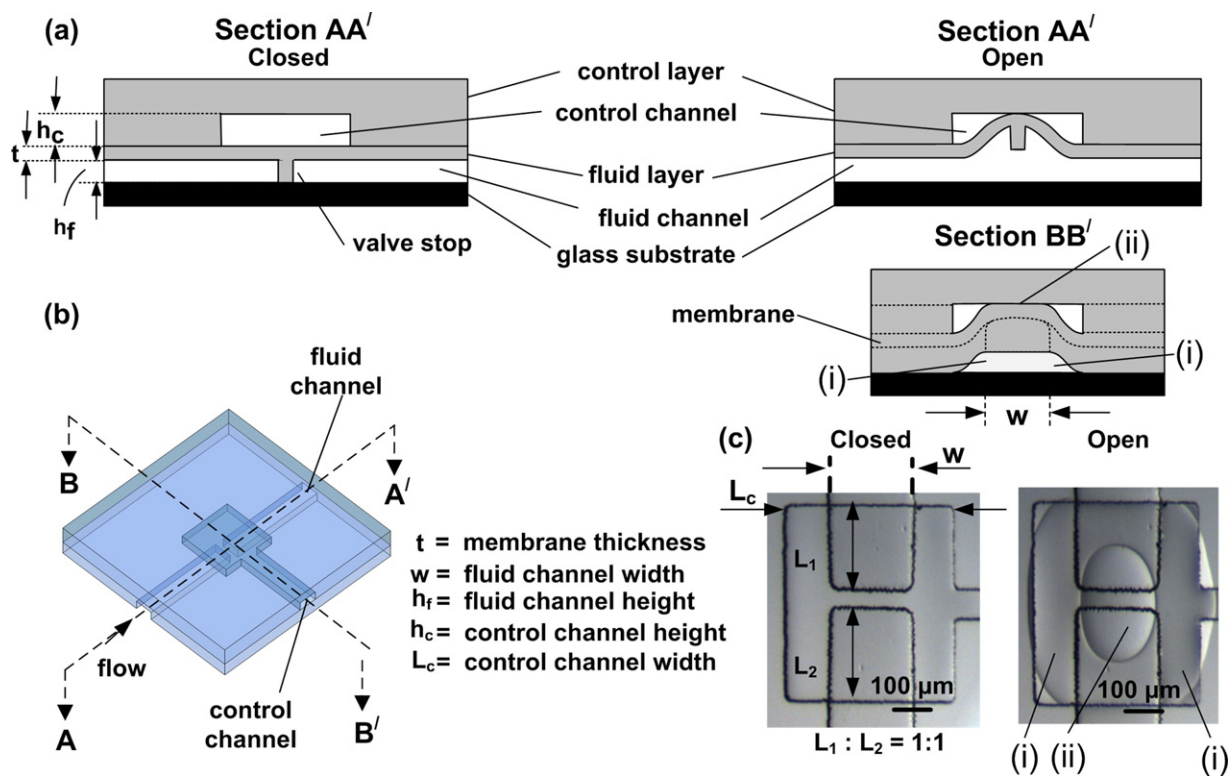


Fig. 1. (a) Cross-sectional and (b) perspective schematic views of a normally closed straight microvalve in closed and open state. (c) Optical micrographs (top view) of a valve in the closed and open state. (i) Indicates the region of the fluid channel that is lifted off the glass substrate, while (ii) indicates the region of the valve that touches the roof of the control channel.

valves were tested without any flow in the fluid channels, and the actuation pressures refer to static values.

3. Results and discussion

3.1. NC microvalve design

To actuate (*i.e.*, open) a NC valve, the membrane that is connected with the valve stop needs to get deflected upwards under the influence of an applied pressure that is lower than ambient (Fig. 1). The key factors that determine the actuation pressure are (a) the mechanical properties of the membrane, and (b) the adhesion forces between the valve stop and the surface it rests against. In turn, these factors depend on a variety of parameters, including the thickness of the membrane, the bulk and surface properties of materials used, and the dimensions of the control and fluid channels.

Fig. 1(a) shows cross-sectional views of a NC valve in the closed and open state. The microvalve consists of a control layer with a channel height (h_c) of 25–50 μm and a fluid layer with a channel height (h_f) of 25–50 μm . The main operational part of the valve consists of a membrane with a thickness (t) of 15–60 μm , and a valve stop with a width of 50 μm to block the flow. Fig. 1(b) shows a perspective view of the NC valve.

Fig. 1(c) shows optical micrographs of a NC valve in the closed and open state. In this figure, the circular or oval-shaped contact area (i) indicates the region of the fluid channel that is lifted off the glass substrate, while (ii) indicates the region of the valve membrane that touches the roof of the control channel. To study the effect of asymmetry on valve performance, we varied two parameters: (1) the shape of the valve stop: straight, diagonal, or v-shaped, and (2) the position of the valve stop within the control chamber, as quantified by the ratio $L_1:L_2$ ranging from 1:1 to 1:5 (Fig. 1(c)). The

rationale behind introducing asymmetry is the creation of a weak point along the contact line of the adhering substrates, so these surfaces can detach from each other more easily upon application of a smaller pressure difference. The width of the fluid channel (w) was also varied from 50 to 350 μm , which is expected to influence the adhesive contact area between the valve stop and the glass substrate, and consequently the actuation pressures. In addition to these operational, often advantageous characteristics, this valve design can be easily fabricated using standard multi-layer soft lithography.

3.2. Effect of various parameters on the actuation pressure of NC valves

3.2.1. Membrane thickness

Membrane thickness influences membrane stiffness, which in turn influences membrane deformation and consequently the actuation pressures. We studied thickness dependence for straight valves only, and the fluid channel width was maintained constant at 175 μm . We observed that the actuation pressures change only marginally (2.4–2.6 psi) for valves with different membrane thicknesses, ranging from 16 to 60 μm . Apparently, other parameters also determine the actuation pressure, in particular adhesion forces (see below). We also observed that the actuation pressures decrease with decrease of the membrane thickness without any glass substrate (Fig. 2). This trend is expected because it is known that the pressure required to deflect membranes increases with increased thickness [24]. Based on the above observations, we conclude that the actuation pressure is primarily governed by the adhesion between the contacting surfaces and not by the membrane stiffness. Since the actuation pressures are not significantly influenced by membrane thicknesses (for the range of values tested here), thicker membranes are preferable, since thinner membranes

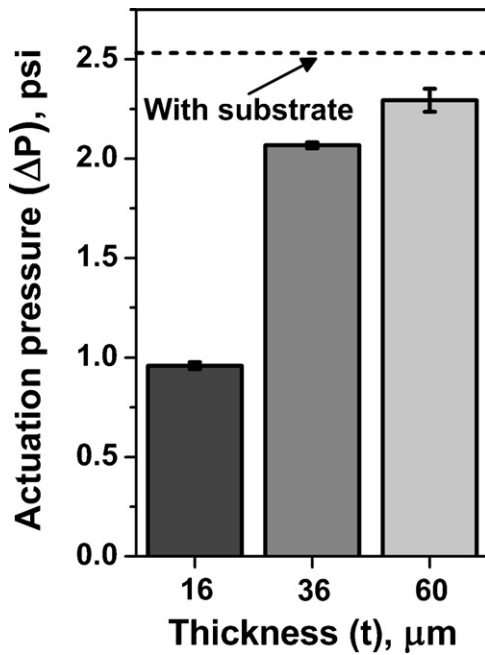


Fig. 2. Effect of thickness of the membrane (t) on actuation pressures, when tested without any substrate. For comparison, we also have included pressure values with a glass substrate. Thicknesses of 16, 36, and 60 μm were tested. Each data point represents the average from experiments on 8 identical valves. Each valve was tested three times.

are susceptible to collapse during fabrication [25] and are usually unreliable during operation (inconsistent actuation pressures). Hence, for all the experiments, we used a membrane thickness of an intermediate value, approximately 36 μm , which yielded reliable valve operation, *i.e.*, variations in actuation pressures for the same valve were within 0.01 psi for different trials.

3.2.2. Fluid channel width

Since adhesion forces were postulated to affect the actuation pressures, fluid channels widths were varied. For all three valve shapes, we observed that the actuation pressures decreased with increasing fluid channel width (Fig. 3). However, the actuation pressures measured for devices without any substrate do not show dependence on width. Hence, the width-dependence of the actuation pressures is primarily due to the adhesion between the valve and the glass substrate. To explain this width-dependence, we derived scaling laws for the actuation pressure based on the peeling of soft rectangular strips from hard substrates (details of this derivation are provided in supplementary information, Section 2). For straight valves, the actuation pressure (ΔP) scales as

$$\Delta P \propto \frac{1}{L_0} + \frac{1}{w}, \quad (1)$$

where w is width of the fluid channel, $2L_0 = L_1 + L_2$ (refer to Fig. 1(c) for definition of L_1 and L_2). Note that L_0 was maintained constant for all the experiments. The width-dependence of actuation pressures can also be explained by considering the area of valve contact with glass, which increases with decreasing width. In this case, it can be shown that the actuation pressure scales as (details of derivation in supplementary information, Section 2).

$$\Delta P \propto 1 - \frac{w}{L_c}, \quad (2)$$

where L_c is the width of the square chamber in the control layer (Fig. 1(c)). We speculate that Eq. (1) (based on peeling) captures the actuation phenomena more accurately compared to Eq. (2) (based on area of contact). In other words, peeling is the more dominant

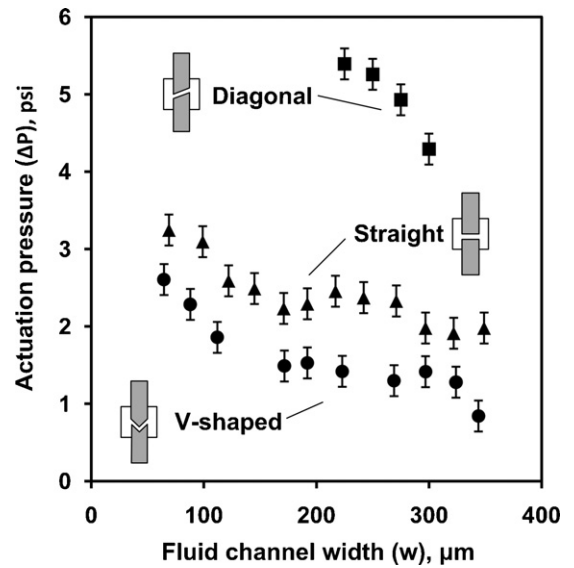


Fig. 3. Actuation pressure for different microvalve shapes (straight, v-shaped, and diagonal) as a function of the width of the fluid channel. Each data point represents the average value from three experiments using the same valve. The errors represented in the plot originate from device-to-device variability, which were a maximum of 0.3 psi for identical valves on 8 different devices.

mode of actuation, and hence, we observe a non-linear decrease in actuation pressures with decreasing channel width. In case of v-shaped and diagonal valves, the corner feature determines the actuation pressure, and hence, Eq. (1) may not be applicable, since the equation is derived on the basis of peeling of a rectangular strip. However, the width-dependence of actuation pressures for these valves can still be explained using Eq. (2).

3.2.3. Shape of the valve stop

As discussed above, asymmetry may reduce actuation pressures because it introduces a weak point in the adhesion between the valve stop and the substrate. One of the ways we introduced asymmetry was by modifying the shape of the valve stop. Fig. 3 shows the experimentally determined actuation pressures as a function of fluid channel width for three different shapes of the valve stop: straight, diagonal and v-shaped. We observed that the actuation pressures were lower for v-shaped valves compared to those for straight valves (Fig. 3). To explain this shape dependence, we describe the actuation of the valve as peeling of a soft adhesive strip (PDMS valve) off a hard substrate (glass). The peeling of the strip (*e.g.*, a scotch tape on a hard substrate) is typically easier from a corner as opposed to peeling from the edge, and hence, the actuation pressures are expected to be lower for v-shaped valves with a corner feature than for straight valves. The lower actuation pressures required for v-shaped valves can be explained semi-quantitatively by considering the relation between the force required to peel (peeling force) and the width of the feature being peeled. Within a first order of approximation, the peeling force is proportional to the width [26,27]. In case of a v-shaped valve, the corner feature results in a very small local width, on the order of the radius of curvature of the corner ($\sim 10 \mu\text{m}$), while for a straight valve, the peeling width is the whole channel width ($\sim 100 \mu\text{m}$). Due to the differences in peeling widths, the actuation pressures for v-shape valves are lower than those for straight ones.

Interestingly, we also observed that the actuation pressures for diagonal valves are higher than those for straight ones, in spite of the presence of a corner feature. This observation mainly results from the fact that for the diagonal valves the corner feature is located away from the central axis. The opening of the valve is

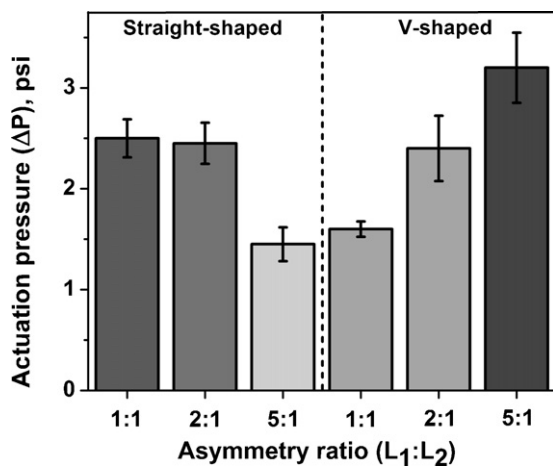


Fig. 4. Effect of asymmetry on actuation pressures for straight and v-shaped valves. Asymmetry ratios tested were 1:1, 2:1, and 5:1.

initiated along the central axis (Fig. 1c), since the valve is least constrained to deflect upwards at the center of the fluid channel. This deflection profile for the valve can be understood in terms of deflection of a fixed-fixed beam [28] (cross-section BB' in Fig. 1(a)). Since valve opening occurs along the central axis of the channel, actuation pressures will be lower only if the peeling forces are small at the center of the valve. In case of diagonal valves, the peeling forces are minimized at the valve edges, and not at the center, thus leading to higher actuation pressures. In contrast, the v-shaped valves have the corner feature along the central axis, and hence actuate at lower pressures. Based on the above discussion, we conclude that the peeling forces should be minimized in the region where the valve opening is initiated to result in lower actuation pressures. A more rigorous explanation for the shape-dependence of actuation pressure based on stress concentration and crack initiation can be found in the [supplementary information, Section 3](#).

3.2.4. Placement of the valve stop

Another way we lowered symmetry in the valve geometry was by varying the position of the valve stop (see Fig. 1) within the control line chamber, which we quantified using the ratio $L_1:L_2$ (Fig. 1(c)). In the case of straight valves, we observed that the actuation pressures were similar for $L_1:L_2$ ratios of 1:1 and 2:1, and decreased for 5:1 ratio (Fig. 4). We attribute this decrease in actuation pressure to the fact that in the latter case one of the membrane lengths is significantly larger than the other. A larger membrane length (L_1 here) will lead to lower stiffness of the corresponding membrane (upper membrane in Fig. 1(c)). As a result, the membrane deflects at a much lower applied pressure and the membrane touches the ceiling of the control channel, as evident from the contact line at the center of the larger membrane in Fig. S7(a). Then, upon the application of additional pressure the outer contact line rapidly propagates, since additional deformation of the membrane, and hence extension of the inner contact line is hindered by contact of the membrane with the ceiling (Fig. S7(b)). We speculate that this rapid propagation of the outer contact line linking the two opposite edges of the valve stop leads to lower actuation pressures for straight valves with $L_1:L_2$ ratios of 5:1.

Interestingly, in case of v-shaped valves, we observed a reverse trend, where the actuation pressures increased when the $L_1:L_2$ ratio was varied as 1:1, 2:1 and 5:1 (Fig. 4). We speculate that as the $L_1:L_2$ ratio increases in v-shaped valves, the axial distance of the shorter side (L_2) is much shorter than in the case of straight valves, due to the presence of the corner feature in v-shaped valves. As a result, the pressure required to deflect the membrane along the

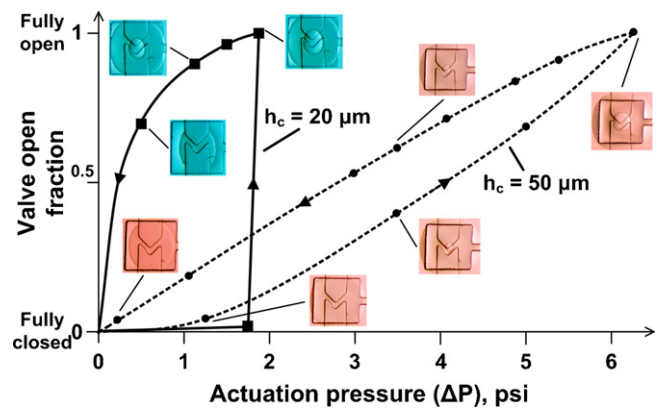


Fig. 5. Semi-quantitative hysteresis plot of actuation pressures for NC valves. Two different heights for the control channel were tested, 20 and 50 μm . The fluid channel width in all the optical micrographs was 175 μm . The valve is considered open when the oval contact line touches the roof of the control channel and the shorter axis of the oval is approximately the size of the fluid channel width (see Fig. 1(c) for open valve). The colors of the optical micrographs have been artificially modified to differentiate the two types of valves. Lines connecting the data points are added to guide the eye.

central axis increases significantly due to the shorter length. Hence, the increase in length of the larger side (L_1) is more than offset by the reduction in length of the shorter side. This effect is more pronounced in v-shaped valves compared to straight valves, since the opening of v-shaped valves is predominantly along the central axis due to the sharp corner feature. Consequently, we observed an increase in actuation pressures with increasing asymmetry in v-shaped valves, due to drastic reduction in the membrane dimension along the central axis. A more rigorous explanation for the asymmetry-dependence of actuation pressure for v-shaped valves based on stress concentration and crack initiation can be found in [supplementary information \(Section 3, Fig. S6\)](#).

3.3. Effect of channel height on hysteresis in valve actuation

Hysteresis becomes important during dynamic, repeated actuation of the valve, since the different pressures required to open and close the valve may lead to temporal delays in operation. Hence, minimizing hysteresis is important for precise control of microfluidic metering and flow control [7]. In NC valves, hysteresis primarily results from the valve membrane adhering to the roof of the control channel in the open state, which is illustrated by formation of a circular or oval shaped contact line in Fig. 5. The hysteresis of adhesion and detachment of the membrane from the roof, typical during adhesive contact between two elastic surfaces, causes hysteresis in the actuation pressures of these valves.

In Fig. 5, we plot the degree by which the valve opens as a function of actuation pressures, where we define the valve as open when the oval contact line touches the roof of the control channel and the shorter axis of the oval is approximately the size of the fluid channel width; Fig. 1(c) shows an open valve. To estimate the fraction of valve opening, the length of the shorter axis of the oval contact line is compared to that of an open valve. The actuation pressures were higher for the taller control channels, since the valve had to deflect a larger distance upward to touch the roof of the control channel. However, we observed lower hysteresis for the taller control channel, i.e., the ratio of the area enclosed within the curve to the actuation pressure is lower for the taller control channel. We attribute the lower hysteresis to the fact that a taller control channel allows for more relief of the membrane deformation when the pressure is decreased, since the membrane is stretched more in a taller control channel. This additional relief results in easier detachment of the valve membrane from the roof, which leads to

lower influence of the adhesion forces between the membrane and the roof when pressure is decreased. Note that the higher actuation pressure for the device with a taller control channel is mainly due to our definition of an open valve. In reality, devices with taller control channels are preferable since the valve can deflect over larger distances, and hence allow more fluid to pass through the channel in the open state.

3.4. Valve performance in a dense network

In microfluidic devices with dense networks, the actuation pressures increase across a network of serially connected valves, due to leakage or pressure losses associated with increasing channel length. As a model for dense microfluidic network, we tested the performance of NC valves by actuating 44 identical valves in series (a schematic illustration and an actual image of the device is shown in [supplementary information, Fig. S8](#)) and compared the valve performance to those in a device with only 3 valves in series. Additionally, to demonstrate the advantage of valves operating at lower actuation pressures in dense networks, we compared valve performance in devices with v-shaped (lower actuation pressures) and straight valves. The fluid channel width was 175 μm and the $L_1:L_2$ ratio was 1:1. In devices with straight valves, 9 out of the 44 valves did not actuate (maximum pressure applied was 12 psi), however, in devices with v-shaped valves, all of the 44 valves actuated in the range of 2–5 psi. As expected, all the 3 valves in the simpler microfluidic device actuated for both valve shapes. The above experiments demonstrate that optimization of valve geometry to reduce actuation pressures and to ensure reliable actuation is crucial for the design of integrated microfluidic networks that contain NC valves.

3.5. Valve actuation over elongated periods for reversibly and irreversibly bonded devices

Leakage due to weak device-to-substrate bonding presents additional challenges in microfluidics, especially during fluid manipulation. In case of NC valves, the leakage issue becomes even more important due to the requirement of selective bonding, where strong bonding is needed for the channels, while the valves remain non-bonded. Although, Yang et al. [20] and Irimia et al. [18] were able to achieve selective irreversible bonding, their technique required additional fabrication steps, such as patterning of a metallic or polymeric layer at the valve stop. Here, we developed a simpler alternative to selectively bond microfluidic devices with NC valves. Oxygen plasma treatment of glass and PDMS as an irreversible bonding technique has been characterized in previous work before bonding is known to lead to strong irreversible bonding [29]. We utilized this technique to irreversibly bond the PDMS device to glass substrate. To prevent the valves from permanently sealing to glass, we exposed the PDMS and glass surfaces to oxygen plasma and then actuated the valves before bringing the PDMS and glass substrate into contact, so that the valves do not contact the glass. We left the valves actuated for 6–8 h, which was sufficiently long for the PDMS surface to lose its hydrophobicity and consequently, the tendency to irreversibly bond to glass [30]. As a result, the device is irreversibly bonded to the glass substrate, except in the areas where the valve stop contacts the glass.

Since the adhesion forces between glass and PDMS are known to increase with time [31] and hence expected to influence the valve operation, we measured the actuation pressures of reversibly and irreversibly bonded devices with glass substrate over a period of 4 weeks. For these experiments, we used v-shaped valves, $L_1:L_2$ ratio of 1:1, and a channel width of 175 μm . In case of reversibly bonded devices, we observed that the actuation pressures increased with time (4 weeks), if the PDMS device and the

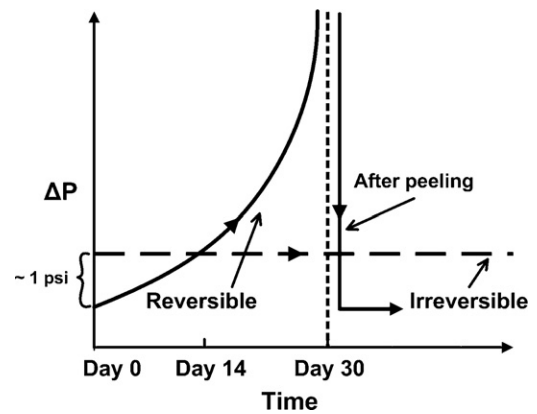


Fig. 6. Qualitative plot showing the effect of device-substrate contact time on actuation pressures for reversibly and irreversibly bonded devices. The dashed vertical line indicates that reversibly bonded device could not be actuated.

glass substrate are maintained in contact, while in case of irreversibly bonded devices, the actuation pressures remained nearly constant over time; a qualitative plot indicating the effect of device-substrate contact time on actuation pressure is shown in [Fig. 6](#). The increase in actuation pressures for reversibly bonded devices can be attributed to time-dependent plastic deformation (creep) of PDMS over micro and nanoscopic features on the glass substrate. This creep-assisted deformation was observed in one study, where PDMS was shown to plastically deform and encapsulate nanoparticles gradually over time [32]. This encapsulation over time will lead to an increase in contact area of the PDMS valve with the glass substrate and hence stronger adhesion, thus resulting in increasing actuation pressures with time. In case of irreversibly bonded devices, however, the actuation pressures remained almost constant over time ([Fig. 6](#)). This behavior is due to the fact that the plasma treatment used for irreversible bonding hardens the PDMS surface by formation of a thin oxide layer (~ 100 nm, small compared to the thickness of the valve membrane) [30], which retards the ability of PDMS to plastically deform.

We also observed that the actuation pressures at the beginning for irreversibly bonded devices are approximately 1 psi higher compared to those for reversibly bonded device ([Fig. 6](#)). The plasma exposure during irreversible bonding decreases the surface roughness of both the PDMS and the glass, which in turn increases the contact area. The increased contact area leads to stronger adhesion, and consequently, higher actuation pressures. However, in the case of reversibly bonded devices, after the PDMS device was peeled off and brought into contact again with the glass substrate, the actuation pressures returned to its original values. We speculate that the peeling of the PDMS breaks the adhesive bonds with the glass surface and new bonds are formed when the PDMS is brought into contact again.

4. Design rules for integrating normally closed microvalves in microfluidic devices

Based on the above experimental results and discussion, we formulate the following set of design rules to integrate NC valves into microfluidic devices:

- (1) *Valve shape.* V-shaped valves are better than straight valves or diagonal valves in terms of actuation pressures and reliability, because they not only actuate at lower pressures than straight for the same fluid channel width, but v-shaped valves also actuate more consistently and their actuation pressure vary less from device to device.

- (2) *Fluid channel width.* Actuation pressures do not significantly change (only 2–3 psi) for a wide range of fluid channel widths (Fig. 3), 50–400 μm . Hence, the NC valves reported in this paper can be used in microfluidic devices with different channel widths.
- (3) *Membrane thickness.* For membrane thicknesses in the range of 15–60 μm , the actuation pressures did not vary significantly (only 1–3 psi). However, thicker membranes are preferable, since valves with thicker membranes actuate more reliably, and valves with thinner membranes are more challenging to fabricate.
- (4) *Position of valve stop.* For straight valves, inducing asymmetry by changing the position of the valve stop reduces actuation pressures, but fabrication limitations might constrain the extent of asymmetry. For instance, in our devices, we could not lower the symmetry in the position of the valve stop beyond a $L_1:L_2$ ratio of 5:1. For v-shaped valves, moving the valve stop does not have a beneficial effect.
- (5) *Hysteresis in valve actuation.* For taller control channels (50 μm), the hysteresis of valve actuation was lower compared to that for shallower channels (25 μm), and hence, taller control channels are preferable, especially for dynamic actuation. Moreover, taller channels allow for more fluid displacement.
- (6) *Bonding.* Selective irreversible bonding will minimize liquid leakage in devices. However, in applications where the PDMS device needs to be peeled off (e.g., when cleaning of the channels is not possible in an assembled device) or the glass substrate cannot be exposed to plasma treatment (e.g., glass surface has been functionalized with oxygen-sensitive chemical groups), then reversible bonding is preferable.

All our experiments were performed with a glass substrate. Since PDMS also adheres well to other materials typically used for microfluidic devices (e.g., PMMA, COC, PC, and PDMS itself), the design rules derived here will also apply to those cases. To demonstrate the application of these NC valves for manipulating liquids, we have added a section to [supplementary information \(Section 6, Fig. S9\)](#), which discusses the use of straight and v-shaped NC valves in a microfluidic chip for metering and mixing of liquids by passive diffusion.

The above analyses and the derived design rules were based on the assumption that adhesion forces between the device and substrate are much larger than the forces required to deflect the membrane. The above assumption is valid for most microfluidic applications because (1) the adhesion forces between device and substrate are high enough to prevent leakage, and (2) the valves are made of soft materials (lower Young's modulus), such as PDMS, to ensure low actuation pressures, and hence the membrane deflection forces will be low. One could encounter a situation in which the forces needed to deflect the membrane become important, for example when adhesion forces have been reduced due to fouling. As a result, the design rules involving factors that contribute significantly to valve stiffness will change. Specifically, the actuation pressures will increase with decreasing fluid channel width and increasing membrane thickness. However, the actuation pressures will not be significantly influenced by the shape of the valve stop and the asymmetry in the position of the valve stop. To investigate how the design rules change when membrane deflection forces dominate, we studied valve actuation in the absence of the bottom glass substrate (thus eliminating the influence of adhesion) using finite element analysis. The results of these studies and an explanation of how the lack of adhesion forces affects the design rules is provided in [Section 7 of the supplementary information](#).

5. Conclusions

In summary, we report a systematic experimental study on the design, fabrication, and operation of NC valves for integration in microfluidic networks. Pneumatic NC valves are increasingly being used in microfluidic devices because they are closed in rest and thus do not require continuous actuation during chemical or biological experiments, while retaining the salient features of the currently more prevalent NO pneumatic valves (simple fabrication and integration). We investigated the effect of various parameters, including channel width, asymmetry (valve geometry and position of the valve stop), and membrane thickness on the actuation pressures and operational reliability of NC valves. We observed that channel width and membrane thickness do not significantly influence the actuation pressures, while introducing valve asymmetry (i.e., the location of weak points of adhesion) lead to a stronger correlation with actuation pressure. From our observations, we showed that the adhesion properties of the valve with the substrate have a stronger influence on the actuation pressure than the mechanical properties of the valve membrane. We also demonstrated that the ability of the NC valves to actuate at lower pressures is significant in dense microfluidic networks, in which multiple valves are typically linked in series. Based on our experimental results and theoretical analysis, we formulated a set of design rules that will guide the design of complex microfluidic networks with NC valves that actuate reliably at low pressures. These design rules for NC valves will benefit their increased use in a wide range of microfluidic applications, especially for those where portability is important. Furthermore, the fact that NC valves require actuation only for filling of a microfluidic device after which all ancillaries can be disconnected, benefits those applications that involve subsequent on-chip analysis of the chemical or biological processes in confined spaces (e.g., fluorescence or Raman microscopy, IR, X-ray).

Acknowledgements

We gratefully acknowledge financial support from the National Science Foundation under awards CMMI 03-28162 and CMMI 07-49028 to Nano-CEMMS; a NanoScience & Engineering Center (NSEC) on Nanomanufacturing. Profilometry was carried out in the Frederick Seitz Materials Research Laboratory Central Facilities, University of Illinois, which is supported in part by the U.S. Department of Energy under grants DE-FG02-07ER46453 and DE-FG02-07ER46471. We also acknowledge Michael Thorson for help with fabrication of the devices.

Appendix A. Supplementary data

Supplementary data associated with this article can be found, in the online version, at [doi:10.1016/j.snb.2011.09.051](https://doi.org/10.1016/j.snb.2011.09.051).

References

- [1] R.G. Blazej, P. Kumaresan, R.A. Mathies, Microfabricated bioprocessor for integrated nanoliter-scale Sanger DNA sequencing, Proceedings of the National Academy of Sciences of the United States of America 103 (2006) 7240–7245.
- [2] C.-C. Lee, G. Sui, A. Elizarov, C.J. Shu, Y.-S. Shin, A.N. Dooley, J. Huang, A. Daridon, P. Wyatt, D. Stout, H.C. Kolb, O.N. Witte, N. Satyamurthy, J.R. Heath, M.E. Phelps, S.R. Quake, H.-R. Tseng, Multistep synthesis of a radiolabeled imaging probe using integrated microfluidics, Science 310 (2005) 1793–1796.
- [3] R. Pal, M. Yang, R. Lin, B.N. Johnson, N. Srivastava, S.Z. Razzacki, K.J. Chomistek, D.C. Heldsinger, R.M. Haque, V.M. Ugaz, P.K. Thwar, Z. Chen, K. Alfano, M.B. Yim, M. Krishnan, A.O. Fuller, R.G. Larson, D.T. Burke, M.A. Burns, An integrated microfluidic device for influenza and other genetic analyses, Lab on a Chip 5 (2005) 1024–1032.
- [4] C.B. Rohde, F. Zeng, R. Gonzalez-Rubio, M. Angel, M.F. Yanik, Microfluidic system for on-chip high-throughput whole-animal sorting and screening at subcellular resolution, Proceedings of the National Academy of Sciences of the United States of America 104 (2007) 13891–13895.

- [5] G.T.A. Kovacs, *Micromachined Transducers Sourcebook*, McGraw-Hill, New York, 1998.
- [6] K. Oh, W. C.H. Ahn, A review of microvalves, *Journal of Micromechanics and Microengineering* 16 (2006) R13.
- [7] M.A. Unger, H.-P. Chou, T. Thorsen, A. Scherer, S.R. Quake, Monolithic microfabricated valves and pumps by multilayer soft lithography, *Science* 288 (2000) 113–116.
- [8] P.L. Skouens, *Valve Handbook*, McGraw-Hill Professional Publishing, New York, 1997.
- [9] J.S. Go, S. Shoji, A disposable, dead volume-free and leak-free in-plane PDMS microvalve, *Sensors and Actuators A: Physical* 114 (2004) 438–444.
- [10] S. Lee, W. Jeong, D.J. Beebe, Microfluidic valve with cored glass microneedle for microinjection, *Lab on a Chip* 3 (2003) 164–167.
- [11] B.R. Schudel, C.J. Choi, B.T. Cunningham, P.J.A. Kenis, Microfluidic chip for combinatorial mixing and screening of assays, *Lab on a Chip* 9 (2009) 1676–1680.
- [12] B.R. Schudel, M. Tanyeri, A. Mukherjee, C.M. Schroeder, P.J.A. Kenis, Multiplexed detection of nucleic acids in a combinatorial screening chip, *Lab on a Chip* 11 (2011) 1916–1923.
- [13] E.P. Kartalov, A. Scherer, S.R. Quake, C.R. Taylor, W.F. Anderson, Experimentally validated quantitative linear model for the device physics of elastomeric microfluidic valves, *Journal of Applied Physics* 101 (2007).
- [14] V. Studer, G. Hang, A. Pandolfi, M. Ortiz, W. French Anderson, S.R. Quake, Scaling properties of a low-actuation pressure microfluidic valve, *Journal of Applied Physics* 95 (2004) 393–398.
- [15] W.H. Grover, R.H.C. Ivester, E.C. Jensen, R.A. Mathies, Development and multiplexed control of latching pneumatic valves using microfluidic logical structures, *Lab on a Chip* 6 (2006) 623–631.
- [16] H. Zhao, K. Stanley, Q.M. Jonathan Wu, E. Cyszewska, Structure and characterization of a planar normally closed bulk-micromachined piezoelectric valve for fuel cell applications, *Sensors and Actuators A: Physical* 120 (2005) 134–141.
- [17] B. Bae, J. Han, R.I. Masel, M.A. Shannon, A bidirectional electrostatic microvalve with microsecond switching performance, *Journal of Microelectromechanical Systems* 16 (2007) 1461–1471.
- [18] D. Irimia, M. Toner, Cell handling using microstructured membranes, *Lab on a Chip* 6 (2006) 345–352.
- [19] K. Hosokawa, R. Maeda, A pneumatically-actuated three-way microvalve fabricated with polydimethylsiloxane using the membrane transfer technique, *Journal of Micromechanics and Microengineering* 10 (2000) 415–420.
- [20] Y.-N. Yang, S.-K. Hsiung, G.-B. Lee, A pneumatic micropump incorporated with a normally closed valve capable of generating a high pumping rate and a high back pressure, *Microfluidics and Nanofluidics* 6 (2009) 823–833.
- [21] W.H. Grover, A.M. Skelley, C.N. Liu, E.T. Lagally, R.A. Mathies, Monolithic membrane valves and diaphragm pumps for practical large-scale integration into glass microfluidic devices, *Sensors and Actuators B: Chemical* 89 (2003) 315–323.
- [22] G.S. Fiorini, D.T. Chiu, Disposable microfluidic devices: fabrication, function, and application, *BioTechniques* 38 (2005) 429–446.
- [23] J.S. Kuo, D.T. Chiu, Disposable microfluidic substrates: transitioning from the research laboratory into the clinic, *Lab on a Chip* 11 (2011) 2656–2665.
- [24] S. Timoshenko, S. Woinowsky-Krieger, *Theory of Plates and Shells*, 2nd, McGraw-Hill Book Company, New York, 1959.
- [25] C.H. Mastrangelo, C.H. Hsu, Mechanical stability and adhesion of microstructures under capillary forces. Part II. Experiments, *Journal of Microelectromechanical Systems* 2 (1993) 44–55.
- [26] A.N. Gent, G.R. Hamed, Peel mechanics, *The Journal of Adhesion* 7 (1975) 91–95.
- [27] K. Kendall, Thin-film peeling—the elastic term, *Journal of Physics D: Applied Physics* 8 (1975) 1449.
- [28] S. Timoshenko, *Strength of Materials*, 3rd ed., Krieger Publishing Company, 1983.
- [29] Y. Xia, G.M. Whitesides, Soft lithography, *Angewandte Chemie International Edition* 37 (1998) 550–575.
- [30] H. Hillborg, J.F. Ankner, U.W. Gedde, G.D. Smith, H.K. Yasuda, K. Wikström, Crosslinked polydimethylsiloxane exposed to oxygen plasma studied by neutron reflectometry and other surface specific techniques, *Polymer* 41 (2000) 6851–6863.
- [31] P.A. Willis, F. Greer, M.C. Lee, J.A. Smith, V.E. White, F.J. Grunthaler, J.J. Sprague, J.P. Rolland, Monolithic photolithographically patterned Fluorocur™ PFPE membrane valves and pumps for in situ planetary exploration, *Lab on a Chip* 8 (2008) 1024–1026.
- [32] L.P. Demejo, D.S. Rimal, J.H. Chen, R.C. Bowen, Time dependent adhesion induced phenomena: the flow of a compliant silicone-polyester copolymer substrate over rigid micrometer size gold and polystyrene particles, *The Journal of Adhesion* 48 (1995) 47–56.

Biographies

Ritika Mohan received her BS degree in Chemical Engineering from the University of Arizona, Tucson. She is currently pursuing her PhD in Chemical & Biomolecular Engineering at the University of Illinois, Urbana-Champaign. Her research efforts are in the area of microfluidics, including the development of pneumatically normally closed microvalves for integrated microfluidics and microfluidic devices for biomedical applications, including screening cells for antibiotic resistance.

Benjamin R. Schudel received his BS degree in Chemical Engineering from the University of Rochester, and his MS and PhD degrees from the University of Illinois at Urbana-Champaign. His research at Illinois focused on developing microfluidic platforms for high-density biological screening applications including protein inhibition and virus identification. Currently he is a postdoctoral researcher at Sandia National Laboratory where he is working on genetic screening platforms for virus studies.

Amit V. Desai received his BTech and MTech degrees in Mechanical Engineering from the Indian Institute of Technology (IIT), Bombay, and his PhD degree in Mechanical & Nuclear Engineering from the Pennsylvania State University in the field of nanomechanics. He is currently a postdoctoral researcher in University of Illinois, Urbana-Champaign, where his research focuses on the application of microfluidic technologies for life-science and biomedical applications, and development of electrostatic valves for integrated microfluidics.

Joshua D. Yearsley participated in a research internship at Sandia National Laboratories before graduating with a BS in Materials Science and Engineering from Rutgers University. Currently he is pursuing his PhD degree at the Pennsylvania State University. His current research focuses on the development of ohmic contacts to III–V high electron mobility transistors.

Christopher A. Applett received his BS in 1988 and his PhD in 1992 from Rensselaer Polytechnic Institute in Materials Engineering, studying the microstructure evolution of transition metals in hydrogen for passivation applications. He joined Sandia National Laboratories in 2000, and focused on developing miniature power sources. His current interests are in the application of microscale systems for power generation, electronics, and microfluidics.

Paul J.A. Kenis received his PhD in Chemical Engineering from Twente University, The Netherlands. After a postdoc at Harvard University he joined the University of Illinois where he is currently a Professor and Head of the department of Chemical & Biomolecular Engineering, with affiliate appointments in the Beckman Institute, the Institute for Genomic Biology, the Frederick Seitz Material Research Laboratory, the Micro- & Nanotechnology Laboratory, and the departments of Bioengineering and Mechanical Science & Engineering. His research efforts include the development of microchemical systems: membraneless microfuel cells, microreactors (e.g. radio-labeling of biomolecules), microfluidic chips for pharmaceutical and (membrane) protein crystallization, platforms for biological cell studies (regenerative biology), sensors and valves for integrated microfluidic networks, and micro/nanofluidic tools for nanomanufacturing.